CHINESE OPTICS LETTERS

Vol. 20, No. 5 | May 2022

$VO_x/NaVO_3$ nanocomposite as a novel saturable absorber for passive *Q*-switching operation

Linghao Kong (孔令豪)[1], Hongwei Chu (褚宏伟)[1*], Na Li (李 娜)[2], Han Pan (潘 瀚)[1], Shengzhi Zhao (赵圣之)[1], and Dechun Li (李德春)[1**]

[1] School of Information Science and Engineering, Shandong University, Qingdao 266237, China

[2] School of Physics and Technology, University of Jinan, Jinan 250022, China

*Corresponding author: hongwei.chu@sdu.edu.cn

**Corresponding author: dechun@sdu.edu.cn

Received January 7, 2022 | Accepted February 18, 2022 | Posted Online March 10, 2022

We report $VO_x/NaVO_3$ nanocomposite as a novel saturable absorber for the first time, to the best of our knowledge. The efficient nonlinear absorption coefficient and the modulation depth are determined by the Z-scan technology. As a saturable absorber, a passively *Q*-switched Nd-doped bulk laser at 1.34 μm is demonstrated, producing the shortest pulse duration of 129 ns at a repetition rate of 274 kHz. In the passively *Q*-switched Tm:YLF laser with the prepared saturable absorber, the shortest pulse duration was 292 ns with a repetition rate of 155 kHz. Our work confirmed the saturable absorption in $VO_x/NaVO_3$ for possible optical modulation in the near-infrared region.

Keywords: nonlinear optical properties; saturable absorber; $VO_x/NaVO_3$ composite; *Q*-switching.

DOI: 10.3788/COL202220.051601

1. Introduction

Pulsed lasers operating in the near-infrared (NIR) region are of great importance in fields such as optical communications, imaging, and material processing[1–3]. Owing to the compactness, high efficiency, and low cost, passively *Q*-switched lasers are an ideal technology to achieve pulsed lasers in the nanosecond level[4]. As a common optical modulator, the saturable absorber is an essential device for the optical pulse generation. In decades, with the development of graphene[5], two-dimensional (2D) materials have been a hot research topic as a saturable absorber to enable *Q*-switching and mode-locking operations. In comparison with the conventional bulk saturable absorber and ultra-long-period grating[6], 2D materials possess unique advantages such as short relaxation time, efficient broadband optical response, and low cost[7–11]. Indeed, black phosphorus (BP)[12], topological insulators (TIs)[13], transition metal oxides (TMOs)[14], transition metal dichalcogenides (TMDs)[15], MXenes[16], and metal-organic frameworks (MOFs)[17] can be applied as the saturable absorber in versatile laser systems. However, these saturable absorbers still suffer some disadvantages.

As a binary TMO, vanadium oxides (VO_x) are of great interest because they possess controllable electronic and optical properties[18,19]. As a typical VO_x, vanadium pentoxide (V_2O_5) suffers from low electronic conductivity and structural instability[20,21]. To overcome the low stability and electronic conductivity, other metal cations are introduced into the V_2O_5 interlayer, since those ions can act as “pillars” to improve structural stability and provide a fast diffusion path[21–23]. Recently, sodium metavanadate ($NaVO_3$) is proposed to boost the charge transfer[23]. On the other hand, the bandgap of V_2O_5 is roughly 2.3 eV[24,25], which cannot absorb the NIR photons, while the bandgap of VO_x with other oxidation states such as VO_2, V_2O_3, and V_3O_5 could be metallic[25], which can absorb the photons within the full optical span.

Researchers have proposed the composite strategy to boost the nonlinear optical properties[25–27]. Up to date, a lot of hybridized saturable absorbers were prepared with graphene-Bi_2Te_3[28], MoS_2-Sb_2Te_3-MoS_2[29], and Fe_3O_4-MXene[30–32], clearly showing the enhanced saturable absorption. In fact, the polyaniline (PANI)/$NaVO_3$ composite was prepared to obtain the large permittivity as well as the optical absorption[33]. Thus, $VO_x/NaVO_3$ composite is expected to enhance the optical features.

In this Letter, to study the nonlinear optical properties of the $VO_x/NaVO_3$ composite material, we used the open-aperture Z-scan technique and measured the effective absorption coefficient, modulation depth, and saturation light intensity at 1.3 and 2 μm. The large modulation depth of 13% at 1.3 μm and the good effective nonlinear absorption coefficient of 0.81 cm/GW at 2 μm were shown. These results revealed that the composite material was a good saturable absorber for pulse manipulation. Subsequently, a passively *Q*-switched laser was operated by using $VO_x/NaVO_3$ as a saturable absorber. When the operating wavelength was 1.3 μm, the shortest pulse width was 129 ns, and the maximum repetition rate was 274 kHz. Our work confirmed that $VO_x/NaVO_3$ composite material could be a promising broadband nonlinear material for ultrafast photonics.

2. Materials and Methods

We took V_2O_3 powder and $NaVO_3$ powder with a mole ratio of 2:3 as the raw materials. After completely ball-milling together, $V_2O_3/NaVO_3$ powder was dispersed in N-methyl-2-pyrrolidone (NMP) and ultrasonically bathed for 6 h. The dispersion solution was centrifuged at 3000 r/min for 15 min. Next, the centrifuged supernatant was dropped slowly onto a quartz substrate with a pipette. The quartz substrate was sucked onto the spinner to ensure that the supernatant was evenly covered on the quartz substrate. Then, the sample was placed in a vacuum drying oven at 80°C for 4 h. Finally, the uniform $V_2O_3/NaVO_3$ nanocomposite was prepared as a thin membrane.

3. Experiment and Results

The morphology and structure of the $VO_x/NaVO_3$ composite material were studied by different characterization methods. Figure 1(a) shows an image of the scanning electron microscope (SEM), showing the small flake-like shape. Figures 1(b)–1(d) illustrate the energy dispersive spectrometer (EDS) elemental mappings of O, V, and Na, respectively, which display that the element distribution was uniform. A high-resolution transmission electron microscope (HRTEM) picture is shown in Fig. 1(e). The lattice plane separation was 0.3447 nm, corresponding to the ($\bar{2}20$) crystal plane separation (0.3439 nm) of $NaVO_3$. In the selected area electron diffraction (SAED) pattern of Fig. 1(f), d1 was 0.325 nm, d2 was 0.185 nm, and d3 was 0.145 nm, corresponding to the (121), (013), and (512) crystallographic planes of $NaVO_3$, respectively. Figure 1(g) shows the X-ray diffraction (XRD) pattern of the $VO_x/NaVO_3$ composite material. The diffraction peaks of V_2O_3 (PDF#34-0187) were marked with asterisks, $NaVO_3$ (PDF#32-1197) with circles, and V_3O_5 (PDF#38-1181) with rhombus. It can be seen from the XRD pattern that VO_x and $NaVO_3$ were well composited. Figure 1(h) clearly shows the six Raman peaks of the $VO_x/NaVO_3$ composite material. The previously reported vibration modes of $NaVO_3$ were consistent with 170.9 cm^{-1}, 348.3 cm^{-1}, and 631.1 cm^{-1}[34]. The same vibration modes of V_2O_3 and $NaVO_3$ were at 242.9 cm^{-1} and 507.3 cm^{-1}[34–36]. The vibration mode of V_3O_5 was classified as 422.3 cm^{-1}[37]. The above characterization techniques presented the morphology and structure of $VO_x/NaVO_3$ composite material, which fully verified the effective composite of VO_x and $NaVO_3$.

Subsequently, the nonlinear optical properties of $VO_x/NaVO_3$ composite were measured by the conventional open-aperture Z-scan technique. The excitation sources were home-made actively *Q*-switched lasers emitting the pulse duration of 50 ns with a repetition rate of 800 Hz at 1.3 and 2 μm, respectively. A convex lens with a focal length of 100 mm was applied to converge the optical beam. Figure 2 displays the typical nonlinear transmission curves versus the relative distance to the focal lens (*Z*) with both excitation wavelengths. Clearly, the $VO_x/NaVO_3$ composite performed the nonlinear saturable absorption. The transmission curve can be fitted by[38]

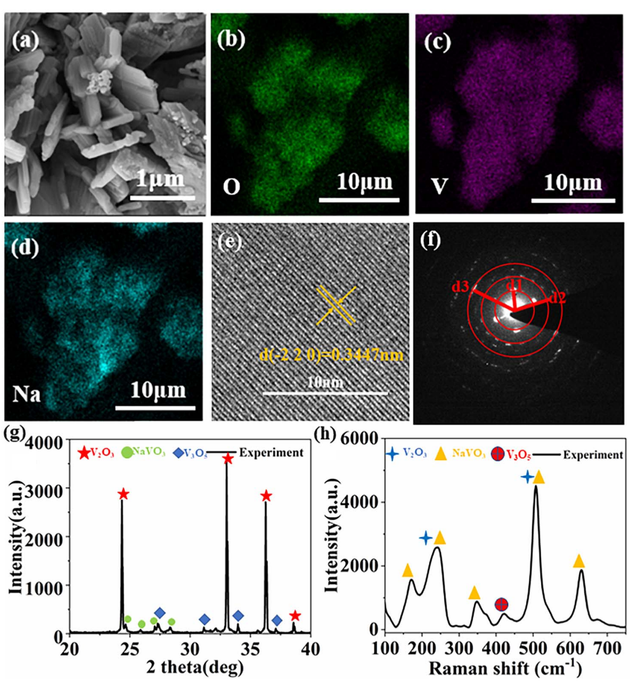

Fig. 1. $VO_x/NaVO_3$ composite material characterization: (a) SEM; (b) O elemental mapping; (c) V elemental mapping; (d) Na elemental mapping; (e) HRTEM; (f) SAED pattern; (g) XRD pattern; and (h) Raman spectrum.

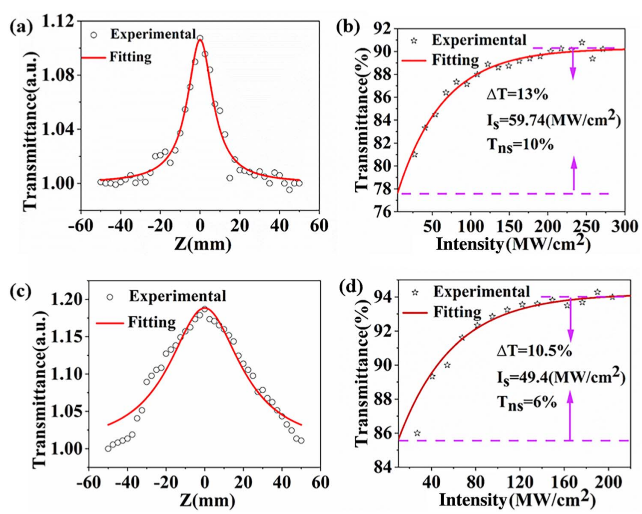

Fig. 2. Nonlinear transmission of VO_x/V_2O_3 nanocomposite versus (a) *Z* axis at 1.3 μm, (b) intensity at 1.3 μm, (c) *Z* axis at 2 μm, and (d) intensity at 2 μm.

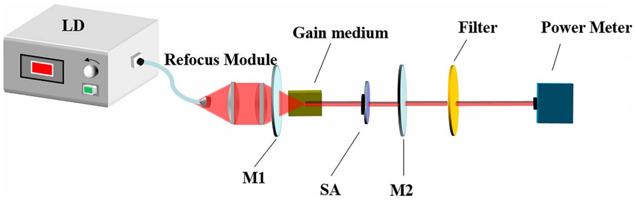

Fig. 3. Schematic setup for the Q-switching operations at 1.3 and 2 μm with $VO_x/NaVO_3$ saturable absorber (gain: $NdVO_4$ for 1.3 μm and Tm:YLF for 2 μm, SA: $VO_x/NaVO_3$).

$$T = \sum_{m=0}^{\infty} \frac{[-q_0(z,0)]^m}{(m+1)^{1.5}}, \qquad m \in N,$$
$$q_0(z,0) = \frac{\beta_{\text{eff}} L_{\text{eff}} I_0}{1+\frac{z^2}{z_0^2}}, \tag{1}$$

where β_{eff} is the effective nonlinear absorption coefficient, L_{eff} is the effective length of the sample, I_0 is the peak intensity on the axis, and z_0 is the Rayleigh range.

Then, we investigated the variation of the transmittance with the change of laser peak density. The fitting equation of experimental data is as follows[39]:

$$T = 1 - \Delta T \exp\left(-\frac{I}{I_s}\right) - T_{\text{ns}}. \tag{2}$$

Herein, ΔT is the modulation depth, I_s is the saturation intensity, and T_{ns} is the nonsaturable losses. As shown in Fig. 2, as the light intensity incident on the sample increased gradually, the transmittance increased gradually at first and then flattened out gradually. This was because with the increase of incident intensity, the absorption coefficient of composite material decreased and the transmittance no longer increased, that is, the material was bleached.

Table 1 summarizes the nonlinear optical parameters of composite materials at 1.3 and 2 μm. These parameters verified that $VO_x/NaVO_3$ composite material possessed good nonlinear absorption and the potential for optical modulators.

The excellent nonlinear optical absorption response of the $VO_x/NaVO_3$ composite indicated that it could be used as a saturable absorber to generate Q-switched pulses. We demonstrated the passively Q-switched bulk lasers operation at 1.3 and 2 μm with the prepared $VO_x/NaVO_3$ composite as the saturable absorber for the first time, to the best of our knowledge. In this section, a compact and simple plane-plane resonator with a length of 20 mm was set up to realize the Q-switching operations. For the Q-switching operation at 1.3 μm, the laser crystal was an a-cut 1% (atomic fraction) $Nd:GdVO_4$ with dimensions of $3\,\text{mm} \times 3\,\text{mm} \times 10\,\text{mm}$. During the experiment, the laser crystal was maintained at 15°C to efficiently remove the thermal load. A fiber-coupled 808 nm laser diode (LD) was employed as the pump. The output coupler (M2) possessed a partial transmission ratio of 3.8%. The whole configuration of the laser cavity can be seen in Fig. 3.

For the continuous-wave (CW) running at 1.3 μm without the saturable absorber inserted into the cavity, the output power increased almost linearly after the threshold. Under the maximum pump power of 3.43 W, the highest output power was 782 mW. Then, the prepared saturable absorber was inserted into the resonator, and the threshold power for the stable Q-switching operation was 2.75 W. Note that VO_x is metallic, and VO_x can absorb the photons in the NIR region at 1.3 μm as well as 2 μm. With the increased pump power, the photogenerated electrons and holes separated and transferred in the $VO_x/NaVO_3$ nanocomposite, leading to the enhanced nonlinear absorption properties. Until the $VO_x/NaVO_3$ nanocomposite was bleached, when the conduction band was fully occupied by the electrons and the valence band was completely dominated by the holes, further optical absorption became impossible owing to the Pauli blocking principle. The losses can be smaller than the gain in the resonator, generating a giant Q-switched pulse. As shown in Fig. 4(a), at the highest pump level, the maximum output power at 1.3 μm was 79 mW. The low output power of the passive Q-switching operation was attributed to the induced extra loss of the saturable absorber. The pulse duration and repetition rate as functions of the pump level are illustrated in Fig. 4(b). It can be seen that the pulse width monotonically decreased, which can be related to the gain factor, while the corresponding repetition rate monotonically increased. When the

Table 1. Nonlinear Absorption Parameters of $VO_x/NaVO_3$.

Wavelength (μm)	β_{eff} (cm/GW)	ΔT (%)	I_s (MW/cm²)	T_{ns} (%)
1.3	−0.66	13	59.7	10
2.0	−0.81	10.5	49.4	6

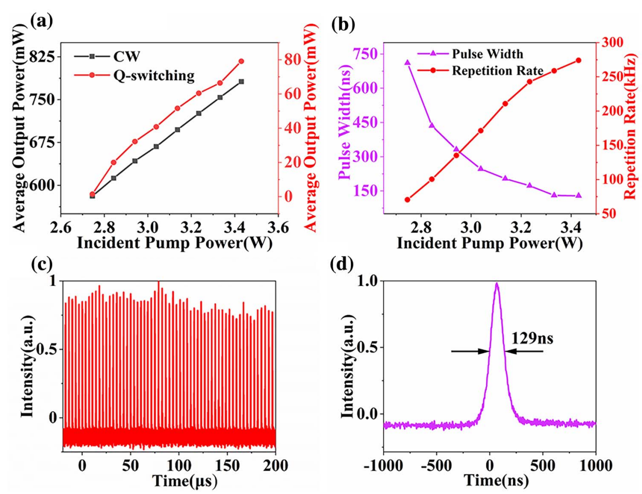

Fig. 4. Passive Q-switching operation at 1.3 μm with $VO_x/NaVO_3$ saturable absorber. (a) CW and Q-switched output power, (b) pulse duration and repetition rate, (c) pulse train, and (d) temporal pulse profile.

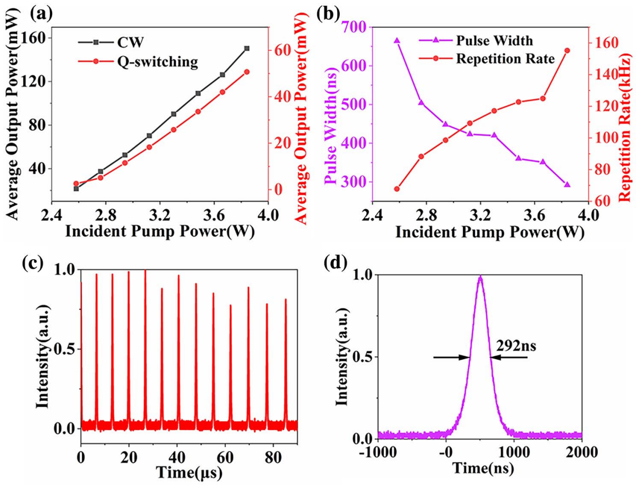

Fig. 5. Passively Q-switched Tm:YLF laser at ~2 μm with $VO_x/NaVO_3$ saturable absorber. (a) CW and Q-switched output power, (b) pulse duration and repetition rate, (c) pulse train, and (d) temporal pulse profile.

incident pump power was 3.43 W, the minimum pulse width was 129 ns, and the maximum repetition rate was 274 kHz. At this time, the pulse train and single pulse profile are shown in Figs. 4(c) and 4(d), respectively. The maximum peak power of Q-switching was 2.24 W, and the corresponding single pulse energy was 289 nJ.

Then, we investigated the nonlinear saturable absorption properties of $VO_x/NaVO_3$ composite at 2 μm. In this section, the laser medium was altered by a 1% (atomic fraction) thulium-doped yttrium lithium fluoride (Tm:YLF) crystal with a length of 8 mm. The pump source was a 794 nm LD with a numerical aperture of 0.22. The pump beam was focused into the laser crystal with a spot size of 400 μm in diameter. The output coupler had a transmission ratio of 5% at 2 μm. In Fig. 5(a), the incident pump power threshold for Q-switched laser output was 2.6 W. When it increased to 3.8 W, the maximum CW and Q-switched output powers were 150.4 mW and 50.7 mW, respectively. The small gain of Tm:YLF and the large loss induced by the saturable absorber resulted in the low output power. Meanwhile, as shown in Fig. 5(b), the minimum pulse width was 292 ns, and the maximum repetition rate was 155 kHz. Figure 5(c) shows the corresponding pulse train diagram, and Fig. 5(d) displays the corresponding single pulse. The corresponding highest peak power was 1.1 W, and the maximum single pulse energy was 327 nJ.

Table 2. Comparison of Passive Q-Switching Performance Parameters of Different SAs at 1.3 and 2 μm.

SA	Crystal	λ [μm]	Width [ns]	Rate [kHz]	Ref.
BP	$Nd:YVO_4$	1.3	72	625	[40]
	$Tm,Ho:LuVO_4$	2	2890	128.4	[41]
MoS_2	Nd:LuAG	1.3	188	73	[42]
	Tm:YAP	2	916	105.1	[43]
Fe_3O_4 at Ti_3C_2	$Nd:YVO_4$	1.3	181	209	[32]
	Tm:YLF	2	320	118	[32]
$VO_x/NaVO_3$	$Nd:GdVO_4$	1.3	129	274	This
	Tm:YLF	2	292	155	work

Table 2 summarizes the passive Q-switching performances with the $VO_x/NaVO_3$ composite saturable absorber and other mainstream saturable absorbers. As shown in Table 2, the composite material can be compared with the mature nanomaterial-based saturable absorbers, indicating that $VO_x/NaVO_3$ composite is a promising nonlinear optical material for ultrafast photonic applications.

4. Conclusion

In summary, the $VO_x/NaVO_3$ composite material was synthesized and characterized. We used the open-aperture Z-scan technique to investigate the nonlinear absorption properties of $VO_x/NaVO_3$ saturable absorber. The composite material displayed a large modulation depth and a high effective nonlinear absorption coefficient for pulsed laser generation. Using $VO_x/NaVO_3$ composite saturable absorber, the passively Q-switched $Nd:GdVO_4$ and Tm:YLF lasers were realized for the first time, to the best of our knowledge, emitting the shortest pulse duration of 129 ns. These results indicated that $VO_x/NaVO_3$ composite could be a promising optical modulation device in ultrafast photonics.

Acknowledgement

This work was supported by the National Natural Science Foundation of China (Nos. 12174223, 12004213, 21872084, and 62175128). H. C. thanks the the Young Scholar Program of Shandong University for the financial support.

References

1. K. Scholle, S. Lamrini, P. Koopmann, and P. Fuhrberg, "2 μm laser sources and their possible applications," in *Frontiers in Guided Wave Optics and Optoelectronics* (Intech, 2010), Chap. 21, p. 471.
2. J. Yu, S. Kwon, Z. Petrášek, O. Park, S. Jun, K. Shin, M. Choi, Y. Park, K. Park, H. Na, N. Lee, D. Lee, J. Kim, P. Schwille, and T. Hyeon, "High-resolution three-photon biomedical imaging using doped ZnS nanocrystals," Nat. Mater. **12**, 359 (2013).
3. D. Teixidor, F. Orozco, T. Thepsonthi, J. Ciurana, C. Rodríguez, and T. Özel, "Effect of process parameters in nanosecond pulsed laser micromachining of PMMA-based microchannels at near-infrared and ultraviolet wavelengths," J. Adv. Manuf. Technol. **67**, 1651 (2012).
4. L. Cao, W. Tang, S. Zhao, Y. Li, X. Zhang, N. Qi, and D. Li, "2 μm passively Q-switched all-solid-state laser based on WSe_2 saturable absorber," Opt. Laser Technol. **113**, 72 (2019).
5. Q. Bao, H. Zhang, Y. Wang, Z. Ni, Y. Yan, Z. Shen, K. Loh, and D. Tang, "Atomic-layer graphene as a saturable absorber for ultrafast pulsed lasers," Adv. Funct. Mater. **19**, 3077 (2009).

6. B. Guo, X. Guo, L. Tang, W. Yang, Q. Chen, and Z. Ren, "Ultra-long-period grating-based multi-wavelength ultrafast fiber laser [Invited]," Chin. Opt. Lett. **19**, 071405 (2021).
7. K. Wang, J. Wang, J. Fan, M. Lotya, A. O Neill, D. Fox, Y. Feng, X. Zhang, B. Jiang, Q. Zhao, H. Zhang, J. Coleman, L. Zhang, and W. Blau, "Ultrafast saturable absorption of two-dimensional MoS_2 nanosheets," ACS Nano **7**, 9260 (2013).
8. Y. Ge, Z. Zhu, Y. Xu, Y. Chen, S. Chen, Z. Liang, Y. Song, Y. Zou, H. Zeng, S. Xu, H. Zhang, and D. Fan, "Broadband nonlinear photoresponse of 2D TiS_2 for ultrashort pulse generation and all-optical thresholding devices," Adv. Opt. Mater. **6**, 1701166 (2018).
9. P. Yin, X. Jiang, R. Huang, X. Wang, Y. Ge, C. Ma, and H. Zhang, "2D materials for nonlinear photonics and electro-optical applications," Adv. Mater. Interfaces **8**, 2100367 (2021).
10. Z. Du, T. Zhang, Z. Xie, J. Ning, X. Lü, J. Xu, and S. Zhu, "Enhanced nonlinear optical response of layered $WSe_{1.4}Te_{0.6}$ alloy in 1 μm passively *Q*-switched laser," Chin. Opt. Lett. **17**, 121404 (2019).
11. J. Wu, Y. Gao, X. Li, J. Long, H. Cui, Z. Luo, W. Xu, and A. Luo, "*Q*-switched mode-locked multimode fiber laser based on a graphene-deposited multimode microfiber," Chin. Opt. Lett. **19**, 121402 (2021).
12. X. Ling, H. Wang, S. Huang, F. Xia, and M. Dresselhaus, "The renaissance of black phosphorus," Proc. Natl. Acad. Sci. USA **112**, 4523 (2015).
13. Y. Xia, D. Qian, D. Hsieh, L. Wray, A. Pal, H. Lin, A. Bansil, D. Grauer, Y. Hor, R. Cava, and M. Hasan, "Observation of a large-gap topological-insulator class with a single Dirac cone on the surface," Nat. Phys. **5**, 398 (2009).
14. F. Wang, H. Chen, D. Lan, F. Zhang, Y. Sun, X. Zhang, S. Li, and T. Cheng, "Highly efficient and robust broadband nano-VO_2(M) saturable absorber for nonlinear optics and ultrafast photonics," Adv. Opt. Mater. **9**, 2100795 (2021).
15. M. Chhowalla, H. Shin, G. Eda, L. Li, K. Loh, and H. Zhang, "The chemistry of two-dimensional layered transition metal dichalcogenide nanosheets," Nat. Chem. **5**, 263 (2013).
16. A. Molle, J. Goldberger, M. Houssa, Y. Xu, S. Zhang, and D. Akinwande, "Buckled two-dimensional Xene sheets," Nat. Mater. **16**, 163 (2017).
17. S. Butler, S. Hollen, L. Cao, Y. Cui, J. Gupta, H. Gutiérrez, T. Heinz, S. Hong, J. Huang, A. Ismach, E. Johnston-Halperin, M. Kuno, V. Plashnitsa, R. Robinson, R. Ruoff, S. Salahuddin, J. Shan, L. Shi, M. Spencer, M. Terrones, W. Windl, and J. Goldberger, "Progress, challenges, and opportunities in two-dimensional materials beyond graphene," ACS Nano **7**, 2898 (2013).
18. C. Wu, F. Feng, and Y. Xie, "Design of vanadium oxide structures with controllable electrical properties for energy applications," Chem. Soc. Rev. **42**, 5157 (2013).
19. M. Imada, A. Fujimori, and Y. Tokura, "Metal-insulator transitions," Rev. Mod. Phys. **70**, 1039 (1998).
20. J. Muster, G. Kim, V. Krstić, J. Park, Y. Park, S. Roth, and M. Burghard, "Electrical transport through individual vanadium pentoxide nanowires," Adv. Mater. **12**, 420 (2000).
21. Y. Lu, J. Wu, J. Liu, M. Lei, S. Tang, P. Lu, L. Yang, H. Yang, and Q. Yang, "Facile synthesis of $Na_{0.33}V_2O_5$ nanosheet-graphene hybrids as ultrahigh performance cathode materials for lithium ion batteries," ACS Appl. Mater. Interfaces **7**, 17433 (2015).
22. Y. Xu, X. Han, L. Zheng, W. Yan, and Y. Xie, "Pillar effect on cyclability enhancement for aqueous lithium ion batteries: a new material of β-vanadium bronze $M_{0.33}V_2O_5$ (M = Ag, Na) nanowires," J. Mater. Chem. **21**, 14466 (2011).
23. L. Chen, H. Wu, H. Wang, L. Chen, X. Pu, and Z. Chen, "Tailoring $NaVO_3$ as a novel stable cathode for lithium rechargeable batteries," Electrochim. Acta **307**, 224 (2019).
24. N. Hieu and D. Lichtman, "Bandgap radiation induced photodesorption from V_2O_5 powder and vanadium oxide surfaces," J. Vac. Sci. Technol. **18**, 49 (1981).
25. N. Szymanski, Z. Liu, T. Alderson, N. Podraza, P. Sarin, and S. Khare, "Electronic and optical properties of vanadium oxides from first principles," Comp. Mater. Sci. **146**, 310 (2018).
26. A. Geim and I. Grigorieva, "Van der Waals heterostructures," Nature **499**, 419 (2013).
27. K. Novoselov, A. Mishchenko, A. Carvalho, and A. Castro Neto, "2D materials and van der Waals heterostructures," Science **353**, 461 (2016).
28. J. Lan, J. Qiao, W. Sung, C. Chen, R. Jhang, S. Lin, L. Ng, G. Liang, M. Wu, L. Tu, C. Cheng, H. Liu, and C. Lee, "Role of carrier-transfer in the optical nonlinearity of graphene/Bi_2Te_3 heterojunctions," Nanoscale **12**, 16956 (2020).
29. W. Liu, Y. Zhu, M. Liu, B. Wen, S. Fang, H. Teng, M. Lei, L. Liu, and Z. Wei, "Optical properties and applications for MoS_2-Sb_2Te_3-MoS_2 heterostructure materials," Photonics Res. **6**, 220 (2018).
30. Y. Hu, H. Chu, D. Li, Y. Li, S. Zhao, L. Dong, and D. Li, "Enhanced *Q*-switching performance of magnetite nanoparticle via compositional engineering with Ti_3C_2 MXene in the near infrared region," J. Mater. Sci. Technol. **81**, 51 (2021).
31. Y. Hu, H. Chu, X. Ma, Y. Li, S. Zhao, and D. Li, "Enhanced optical nonlinearities in Ti_3C_2 MXene decorated Fe_3O_4 nanocomposites for highly stable ultrafast pulse generation," Mater. Today Phys. **21**, 100482 (2021).
32. T. Zhang, H. Chu, L. Dong, Y. Li, S. Zhao, Y. Wang, J. Zhou, and D. Li, "Synthesis and optical nonlinearity investigation of novel Fe_3O_4@Ti_3C_2 MXene hybrid nanomaterials from 1 to 2 μm," J. Mater. Chem. C **9**, 1772 (2021).
33. T. Machappa and M. Ambika Prasad, "AC conductivity and dielectric behavior of polyaniline/sodium metavenadate (PANI/$NaVO_3$) composites," Physica B **404**, 4168 (2009).
34. S. Seetharaman, H. L. Bhar, and P. Narayanan, "Raman-spectroscopic studies on sodium meta-vanadate," J. Raman Spectrosc. **14**, 401 (1983).
35. L. Hu, C. Xie, S. Zhu, M. Zhu, and Y. Sun, "Unveiling the mechanisms of metal-insulator transitions in V_2O_3: the role of trigonal distortion," Phys. Rev. B **103**, 085119 (2021).
36. A. Okamoto, Y. Fujita, and C. Tatsuyama, "Raman study on the high temperature transition in V_2O_3," J. Phys. Soc. Jpn. **52**, 312 (1983).
37. P. Shvets, O. Dikaya, K. Maksimova, and A. Goikhman, "A review of Raman spectroscopy of vanadium oxides," J. Raman Spectrosc. **50**, 1226 (2019).
38. H. Pan, H. Chu, Z. Pan, S. Zhao, M. Yang, J. Chai, S. Wang, D. Chi, and D. Li, "Large-scale monolayer molybdenum disulfide (MoS_2) for mid-infrared photonics," Nanophotonics **9**, 4703 (2019).
39. L. Dong, H. Chu, X. Wang, Y. Li, and D. Li, "Enhanced broadband nonlinear optical response of TiO_2 /CuO nanosheets via oxygen vacancy engineering," Nanophotonics **10**, 1541 (2021).
40. X. Sun, H. Nie, J. He, R. Zhao, X. Su, Y. Wang, B. Zhang, R. Wang, and K. Yang, "Passively *Q*-switched Nd:$GdVO_4$ 1.3 μm laser with few-layered black phosphorus saturable absorber," IEEE J. Sel. Top Quantum Electron **24**, 1600405 (2017).
41. L. Li, T. Li, L. Zhou, J. Fan, Y. Yang, W. Xie, and S. Li, "Passively *Q*-switched diode-pumped Tm,Ho:$LuVO_4$ laser with a black phosphorus saturable absorber," Chin. Phys. B **28**, 213 (2019).
42. K. Wang, K. Yang, X. Zhang, S. Zhao, C. Luan, C. Liu, J. Wang, X. Xu, and J. Xu, "Passively *Q*-switched laser at 1.3 μm with few-layered MoS_2 saturable absorber," IEEE J. Sel. Top Quantum Electron **23**, 1600205 (2016).
43. T. Gao, R. Zhang, Z. Shi, Z. Jiang, and J. Cui, "High peak power passively *Q*-switched 2 μm solid-state laser based on a MoS_2 saturated absorber," Microw. Opt. Technol. Lett. **63**, 1990 (2021).